DOI: 10.1002/ejic.200600666

Selective Precipitation of Alkaline Earth Metal Cations with Dipicrylamine Anion: Structure–Selectivity Correlation

Pragati Agnihotri,[a] Subrata Patra,[a] Eringathodi Suresh,[a] Parimal Paul,*[a] and Pushpito K. Ghosh*[a]

Keywords: O ligands / Alkaline earth metals / Selectivity / Structure–selectivity correlation

Salts of dipicrylamine anion and alkaline earth metal ions are highly soluble in water, unlike the salts formed with K^+, Rb^+, and Cs^+. We report here that when DPA^- is added to a solution containing Mg^{2+}, Ca^{2+}, Sr^{2+}, and Ba^{2+}, Ba^{2+} can be precipitated out with high yield and selectivity by optimizing the concentrations. When $[DPA^-] = 0.17$ M and the molar ratio of each metal ion to DPA^- is 1:1, Sr^{2+} and Ba^{2+} are precipitated out in about 90% overall yield (with respect to DPA^-) and 85% selectivity of Ba^{2+}. Salts of Mg^{2+} and Ca^{2+} are virtually absent. Single-crystal XRD of the pure Sr^{2+} and Ba^{2+} compounds has been performed. Layered structures are observed with clear evidence that the salts exist in the form of complexes with the composition $[M(DPA)_2(H_2O)_4]$. This is different to the case of alkali metal ions, where the complexes have no coordinated water molecules. The Ba^{2+} complex has a more compact layered structure than the Sr^{2+} complex, with reduced exposure of the polar entities. As a result it would be expected to have relatively lower solubility in water, which would account for its selective precipitation over the Sr^{2+} complex. That it is legitimate to rationalize the precipitation behavior from the structure deduced by single crystal XRD is verified due to the close similarity between the experimental powder XRD data of the precipitate and the simulated powder XRD pattern obtained from the single-crystal data.

Introduction

Dipicrylamine (2,2′,4,4′,6,6′-hexanitrodiphenylamine, DPA) possesses some interesting structural features (Figure 1), namely six nitro groups that are flexible and can interact and adjust in the space and partial delocalization of the resultant charge mediated by the aromatic rings that facilitates coordination of the oxygen atoms with suitable metal ions. Recently, crystal structures of DPA and a computational study on the intermolecular interactions observed in the crystal structure have been reported.[1] The crystal structures of some of its organic salts have also been reported.[2] DPA^- has been used for quantitative estimation of potassium by Winkel and Mass.[3] It has also been used for the recovery of K^+ from seawater,[4] and recovery of Cs^+ from radioactive waste.[5,6] Studies have also been conducted with a mixture of cations (e.g. K^+, Rb^+, and Cs^+) and DPA^- to assess the relative selectivity of the metal ion.[7] In spite of the voluminous reports on the utility of DPA^-, little is known about the factors that control its selectivity towards different alkali and alkaline earth metal ions. We recently undertook a systematic study with Na^+, K^+, Rb^+, and Cs^+ to understand the factors that control the selective precipitation behavior.[8] By applying this reaction to the complex sea bittern system, highly pure and concentrated aqueous KCl could be extracted and the same KCl solution could be utilized in a novel process for the preparation of potassium sulfate.[9]

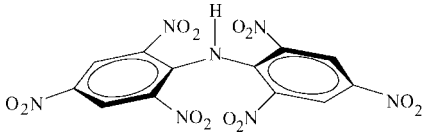

Figure 1. Structure of dipicrylamine (DPA).

Alkaline earth metal ions are dicationic (Mg^{2+}, Ca^{2+}, Sr^{2+}, and Ba^{2+}) and their hydration enthalpies (–459.1, –376.9, –344.9, and –311.9 kcal mol^{-1}, respectively) are significantly higher than those of the alkali metal ions (Na^+: –97, K^+: –77, Rb^+: –70, and Cs^+: –63 kcal mol^{-1}). Because of this difference in ionic charge and hydration enthalpy, their structural network and selective precipitation properties are expected to be significantly different from that of

[a] Analytical Science Division, Central Salt and Marine Chemicals Research Institute, G. B. Marg, Bhavnagar 364002, India
E-mail: ppaul@csmcri.org
pkghosh@csmcri.org

Supporting information for this article is available on the WWW under http://www.eurjic.org or from the author.

the alkali metal ions. Herein, we report our study on the selective precipitation of Ba^{2+} in high yield from a solution containing the DPA^- anion and an equimolar mixture of Mg^{2+}, Ca^{2+}, Sr^{2+}, and Ba^{2+}. This precipitation is induced at high concentrations (ca. 0.15–0.50 M) of DPA^-. We have also isolated single crystals of the Sr^{2+} and Ba^{2+} salts of DPA^- to deduce their structures and to unravel the causes underlining this selective precipitation.

Results and Discussion

Ion Selectivity

Ion selectivity was determined by analyzing the concentrations of metal ions in the precipitate formed upon addition of 1 mL of an aqueous solution containing Mg^{2+}, Sr^{2+}, and Ba^{2+} (0.5 M each) to 2 mL of an aqueous solution containing 0.25 M $Ca(DPA)_2$ to yield the overall composition: 0.333 M DPA^- and 0.166 M each of the four metal ions prior to precipitation. The relative proportions of metal ions in the precipitate were assayed by ion chromatography using a reference standard for the purpose of comparison (Figure 2). The tiny peaks corresponding to Mg^{2+} and Ca^{2+} in the ion chromatogram of the precipitate are possibly due to entrapped impurities in the solid (such impurities can remain since washing was avoided to prevent re-dissolution of the precipitate). The molar percentages of Sr^{2+} and Ba^{2+} in the precipitate were 24.1 and 75.9, respectively, while the total molar yield, i.e. sum of the molar yields of $Sr(DPA)_2$ and $Ba(DPA)_2$, was 91% with respect to DPA^- taken up. When all of the concentrations in the solution were halved, the molar percentages of $Sr^{2+}$and Ba^{2+} in the precipitate were 15.0 and 84.9, respectively, while the total molar yield remained virtually constant at 90%. In other words, there was higher recovery of Ba^{2+} (76% in the latter case relative to 69% in the former case) with enhanced selectivity (84.9% in the latter case relative to 75.9% in the former case). This encouraging trend suggests that further increases in recovery and selectivity of Ba^{2+} are possible, although such optimization studies were not carried out. It has been shown previously that understanding of the structures of the solid-state complexes obtained with alkali metal ions can provide valuable insight into their solubility characteristics and precipitation behavior. To extend this understanding to the present system, $Sr^{2+}$and Ba^{2+} complexes of DPA^- were synthesized and structurally characterized.

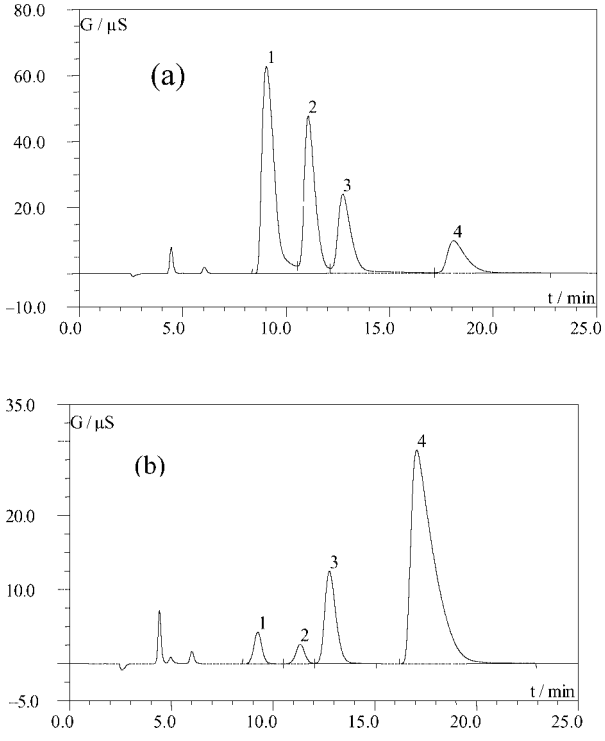

Figure 2. Ion chromatograms of (a) a standard solution containing $MgCl_2$, $CaCl_2$, $SrCl_2$, and $BaCl_2$ (20 ppm each); 1 (Mg^{2+}): 9.037, 2 (Ca^{2+}): 11.067, 3 (Sr^{2+}): 12.740, 4 (Ba^{2+}): 18.090 min; and (b) the precipitate separated from the mixture containing 0.17 M of each metal ion; 1 (Mg^{2+}): 9.247, 2 (Ca^{2+}): 11.333, 3 (Sr^{2+}): 12.777, 4 (Ba^{2+}): 17.070 min. The tiny peaks of Mg^{2+} and Ca^{2+} found in (b) are probably due to trace amounts of these ions trapped in the precipitate as it was not washed with water to avoid dissolution of the complexes.

Synthesis of Complexes

$Sr^{2+}$and Ba^{2+} complexes of DPA^- were synthesized by adding an aqueous solution of 0.2 M $Ca(DPA)_2$ to a 0.2 M aqueous solution of the respective chloride salt ($SrCl_2$ and $BaCl_2$), as described in the Experimental Section. The Sr^{2+} complex was partially precipitated during the reaction, and a second crop of the precipitate was obtained when the volume of the filtrate was reduced; even so, the yield was only 72%. In the case of the Ba^{2+} complex, precipitation was nearly instantaneous and almost quantitative (92%), even without recourse to evaporation, which is clearly indicative of its lower solubility than the Sr^{2+} complex. C, H, and N analyses corresponded to the compositions $[Sr(DPA)_2(H_2O)_4]$ (**1**) and $[Ba(DPA)_2(H_2O)_4]$ (**2**). X-ray quality single crystals of **1** and **2** were grown by slow evaporation of dilute aqueous solutions of the complexes at room temperature, and the molecular structures were established by single-crystal X-ray diffraction (see below). To verify whether the bulk precipitates are structurally similar to the single crystals, powder XRD patterns of the bulk precipitates were recorded and compared to those obtained from the single-crystal X-ray data by simulation. The close similarity between the experimental and simulated diffractograms of both **1** and **2** (Figure 3) led us to conclude that the former are indeed structurally similar to the latter and, therefore, understanding of the crystal structures may provide vital information about the solubility/selectivity trend.

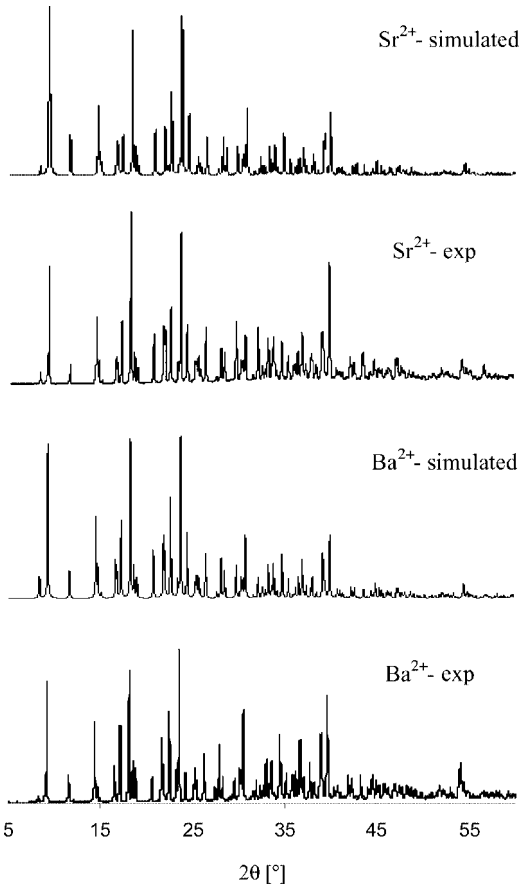

Figure 3. Experimental powder XRD data of bulk precipitates of Sr^{2+} and Ba^{2+} salts of DPA^- vs. XRD patterns simulated from the single-crystal X-ray data of the corresponding crystalline salts grown from the bulk precipitates.

Crystal Structures

[Sr(DPA)$_2$(H$_2$O)$_4$] (1)

This molecule crystallizes in the acentric space group $P322_1$ – the Sr^{2+} atom possesses a twofold symmetry. The Sr^{2+} ion, which occupies a special position, is coordinated to ten oxygen atoms, six oxygen atoms from the nitro groups of four symmetry-related DPA^- moieties and four oxygen atoms from water molecules. An ORTEP view of the binding of DPA^- to the metal ion is available as Supporting Information (Figure S1). Interactions between the DPA^- anion and the metal ions generate a layered, one-dimensional network, as depicted in Figure 4. The Sr···Sr distance is 9.401 Å, and the angle subtended by the metal ions within the layer is 113.89°. The Sr···O distances are in the range 2.785(2)–2.852(2) Å, and the average Sr···O distance is 2.810(2) Å (Table 1). The oxygen atoms of the coordinated water molecules interact even more strongly with the metal ion [Sr···O13 = 2.534(2) and Sr···O14 = 2.595(2) Å]. The Sr···O distances observed from the structural data (Table 1) are in close agreement with the reported values.[10] The phenyl rings of DPA^- in the complex are almost orthogonal to each other, and the mean plane distortion between them is 75.55°. The coordinated *o*-nitro groups N1–O1/O2 and N5–O7/O8 are rotated by 11.98° and 30.66°, respectively, with respect to the phenyl rings to which they are attached. The uncoordinated *o*-nitro groups N3–O5/O6 and N7–O11/O12 also show significant rotation (88.56° and 19.55°, respectively) from the respective phenyl rings (C1–C6 and C7–C12) to which they are attached. The *p*-nitro groups N2–O3/O4 and N6–O9/O10 are almost in the same plane with respect to the phenyl rings C1–C6 and C7–C12 (deviation 0.82° and 0.54°). It appears that these rotations are self-optimized in order to make effective coordination with the metal ion to propagate the doubly bridged Sr^{2+}-DPA^- corrugated network.

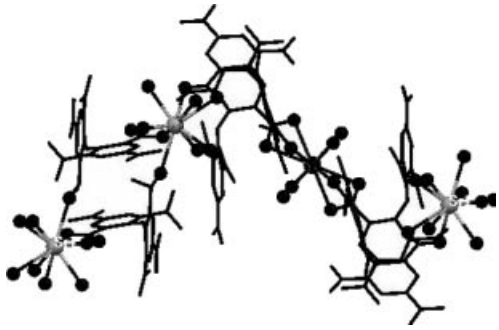

Figure 4. Mercury diagram depicting the adjacent corrugated layered network created by linking of $Sr(H_2O)_4$ units and DPA^-.

Table 1. Metal–oxygen distances [Å] for **1** and **2**.

Compound **1**[a]			
Sr(1)–O(14)#1	2.5340(19)	Sr(1)–O(7)#3	2.785(2)
Sr(1)–O(14)	2.534(2)	Sr(1)–O(2)#1	2.792(2)
Sr(1)–O(13)#1	2.5945(19)	Sr(1)–O(2)	2.792(2)
Sr(1)–O(13)	2.5945(18)	Sr(1)–O(1)#1	2.8523(16)
Sr(1)–O(7)#2	2.785(2)	Sr(1)–O(1)	2.8523(17)
Compound **2**[b]			
Ba–O(14)#1	2.791(2)	Ba–O(3)#2	2.991(2)
Ba–O(14)	2.791(2)	Ba–O(3)#3	2.991(2)
Ba–O(13)#1	2.845(2)	Ba–O(1)#4	2.993(2)
Ba–O(13)	2.845(2)	Ba–O(1)#5	2.993(2)
Ba–O(7)#1	3.051(2)	Ba–O(2)#4	3.120(2)
Ba–O(7)	3.051(2)	Ba–O(2)#5	3.120(2)

[a] #1: $x - y, -y, -z + 7/3$; #2: $-x + y, -x, z + 1/3$, #3: $y, x, -z + 2$, #4 $-y, x - y, z - 1/3$. [b] #1: $x + 1, -y + 1, -z + 2$; #2: $x + 2, -y, -z + 2$; #3: $x - 1, y + 1, z$; #4: $x - 1, y, z$; #5: $-x + 2, -y + 1, -z + 2$.

The molecular packing shows strong intermolecular O–H···O interactions. The hydrogen atoms of the symmetrically disposed coordinated water molecules (H131 and H132 attached to O13, and H141 and H142 attached to O14) on either side act as donors and participate in H-bonding with the nitro oxygen atoms O5, O9, O3, and O12 to bridge the adjacent corrugated layers into a two-dimensional H-bonded network. The nitro oxygen atom O10 is also involved in an intermolecular C–H···O interaction with the phenyl hydrogen H4. Details of the hydrogen-bonding parameters are given in Table 2.

Table 2. Hydrogen-bonding parameters for **1** and **2**.

D–H···A	*d*(D···A) [Å]	<D–H···A [°]
	Compound **1**[a]	
O(13)–H(131)···O(5)#1	O(13)···O(5) = 2.089(4)	O(13)–H(131)···O(5) = 152
O(13)–H(132)···O(9)#2	O(13)···O(9) = 2.944(4)	O(13)–H(131)···O(5) = 145
O(14)–H(141)···O(3)#3	O(14)···O(3) = 2.920(4)	O(14)–H(141)···O(3) = 151
O(14)–H(142)···O(12)#4	O(14)···O(12) = 3.085(4)	O(14)–H(142)···O(12) = 174
C(4)–H(4)···O(10)#5	C(4)···O(10) = 3.221(4)	C(4)–H(4)···O(10) = 134
	Compound **2**[b]	
O(13)–H(131)···O(8)#1	O(13)···O(8) = 3.145(3)	O(13)-(131)···O(8) = 150(4)
O(13)–H(132)···O(9)#2	O(13)···O(9) = 2.901(4)	O(13)-(131)···O(9) = 170(5)
O(14)–H(141)···O(11)#3	O(14)···O(11) = 3.024(4)	O(14)–H(141)···O(11) = 138(6)
O(14)–H(141)···O(4)#4	O(14)···O(4) = 3.109(3)	O(14)–H(141)···O(4) = 140(6)
O(14)–H(142)···O(10)#5	O(14)···O(10) = 3.060(3)	O(14)–H(142)···O(10) = 159(5)

[a] #1: *y*, –1 + *x*, 2 – *z*; #2: 1 + *y*, *x*, 2 – *z*; #3: –1 + *x*, –1 + *y*, *z*; #4: *y*, –1 + *x*, 2 – *z*; #5: 1 + *x*, 1 + *y*, *z*. [b] #1: *x*, *y*, *z*; #2: *x*, –1 + *y*, *z*; #3: –1 + *x*, *y*, 1 + *z*; #4: 2 – *x*, –*y*, 2 – *z*; #5: 1 – *x*, 2 – *y*, 2 – *z*.

[Ba(DPA)$_2$(H$_2$O)$_4$] (2)

The metal ion in compound **2** sits on a center of symmetry and can accommodate twelve coordinating atoms (eight nitro oxygen atoms from six surrounding DPA$^-$ moieties and four oxygen atoms from coordinated water molecules). An ORTEP view of the binding of DPA$^-$ to the metal ion is available as Supporting Information (Figure S2). The Ba···O distances involving the nitro oxygen atoms are in the range 2.991–3.120 Å (Table 1; average Ba···O = 3.0386 Å). The Ba···O distances involving O13 and O14 of the water molecules are 2.845 and 2.791 Å, respectively, which are in close agreement with the reported values.[11] The Ba···O interaction involving the nitro oxygen atoms O1, O2, and O3 creates a layered doubly bridged architecture in the *ab* plane. However, an additional short contact formed by the nitro oxygen O7 from either side bridges the neighboring layers and extends the layered motif into a two-dimensional sheet-like arrangement, as depicted in Figure 5. The Ba···Ba distance within the coordination network is 9.189 and 6.635 Å along the *a* and *b* axes, respectively. The mean plane distortion between the phenyl rings of DPA$^-$ is 71.78°, which is 3.77° less than that in complex **1**. The coordinated *o*-nitro groups N1–O1/O2 and N5–O7/O8 are rotated with respect to the phenyl rings to which they are attached by 15.49° and 10.06°, respectively, whereas the coordinated *p*-nitro group N2–O3/O4 shows a comparatively smaller rotation (4.68°) with respect to the phenyl ring C1–C6. The uncoordinated *o*-nitro groups N3–O5/O6 and N7–O11/O12 and the *p*-nitro group N6–O9/10 make angles of 29.17°, 5.39°, and 4.35° with respect to the phenyl rings to which they are attached.

Analysis of the molecular packing reveals that both the hydrogen atoms from all the coordinated symmetry-related water molecules act as donors and are involved in intra- and intermolecular O–H···O interactions with the nitro oxygen atoms. Details of the hydrogen-bonding parameters are given in Table 2. These intermolecular H-bonding interactions not only connect the adjacent two-dimensional sheets but also stabilize the network in the crystal lattice.

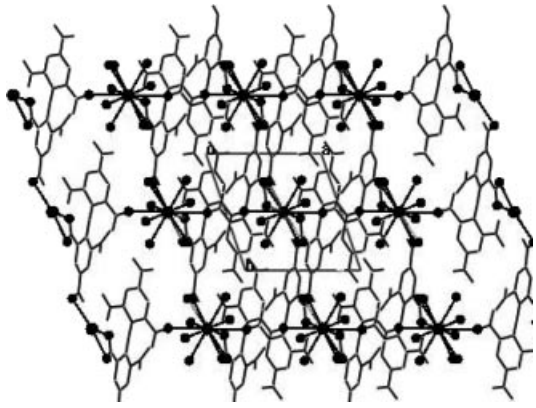

Figure 5. Packing diagram (Mercury) viewed down the *c* axis showing the two-dimensional coordination networks in complex **2**.

Structure–Selectivity Correlation

Competitive precipitation of a metal ion from a mixture of cations determines selectivity. Sr^{2+} and Ba^{2+} complexes with DPA$^-$ have identical compositions, therefore selective precipitation of a particular complex should be related to the structural arrangement in the solid state, which can profoundly influence the solubility in water. As can be seen from the single-crystal structures of **1** and **2**, these structures are held in place by M···O and C–H···O interactions that form an extended network. From the packing diagrams it is clear that the metal ions are encapsulated in the cavities at regular intervals in the structural network. This self-assembled system reduces the solubility of the complex, and consequently precipitation occurs. Space-filling models of the respective cavities comprising the metal ion and metal-bound oxygen atoms have been generated from the packing diagrams of **1** and **2** (Figure 6 and Figure 7, respectively). The ten oxygen atoms around Sr^{2+} and the twelve oxygen atoms around Ba^{2+} form near-spherical cavities, the approximate diameter of which can be determined from the average distance between the *trans* oxygen atoms having O–M–O angles ≤ 150°. The approximate diameters of the

cavities thus obtained are 5.43 and 6.08 Å for Sr^{2+} and Ba^{2+}, respectively. These diameters qualitatively follow the order of the ionic sizes of these cations (2.26 and 2.68 Å for Sr^{2+} and Ba^{2+}, respectively).[12] $Mg^{2+}$and Ca^{2+}, with ionic sizes of 1.30 and 1.98 Å, respectively, may be too small to fit in this cavity and make the significant M···O interactions needed to form a stable assembly, provided a similar structure were to apply in their case also. Alternative structures with smaller cavity sizes are, of course, possible with a lower number of ligands around the metal ion with reduced steric hindrance. However, due to the lack of a sufficient number of M···O and intermolecular C–H···O interactions for such an arrangement, it may not be possible to form the stable assembly essential for precipitation. In the case of alkali metal ions, Na^+, which has a smaller ionic size (1.94 Å), does not precipitate out in the presence of DPA^- either due to the lack of formation of a supramolecular network. However, K^+, Rb^+, and Cs^+, which have ionic sizes of 2.66, 2.94, and 3.34 Å, respectively, precipitate out spontaneously in the presence of DPA^-.[8] Therefore, the size of the cation is an important factor for the formation of the network structure and thus precipitation.

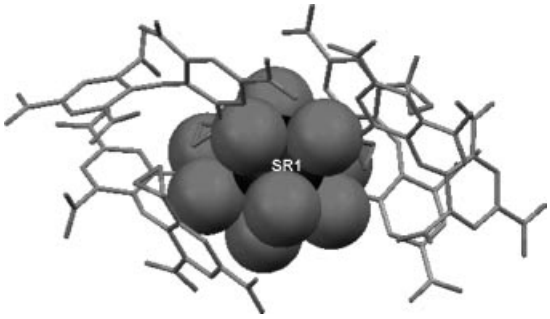

Figure 6. Space-filling model (Mercury diagram) of the cavity comprising the Sr^{2+} ion and metal-bound oxygen atoms.

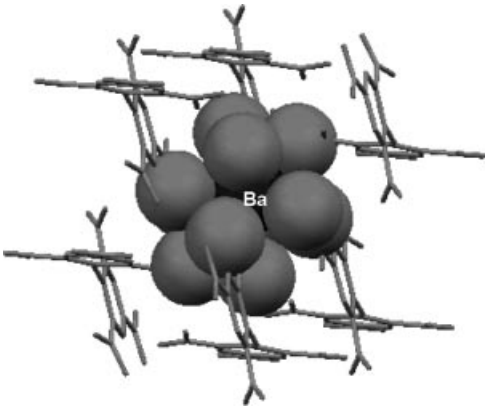

Figure 7. Space-filling model (Mercury diagram) of the cavity comprising the Ba^{2+} ion and metal-bound oxygen atoms.

There can be variations in solubility even for complexes exhibiting a network structure. Reduced exposure of the metal ion and the polar groups of the ligand to water (by tying these up internally in the structure) would lead to reduced solubility and, consequently, more favorable precipitation. In the Ba^{2+} complex, the metal ion is twelve coordinate, unlike in the case of the Sr^{2+} complex in which the coordination number is 10. Moreover, analysis of the packing diagram shows that H-bonding interactions connect the adjacent two-dimensional sheets, which makes the structure more compact than that of the Sr^{2+} complex and reduces the possibility of contact between the polar groups of the ligand and/or coordinated water molecules with the solvent (water). The higher expected stability of the network (Figure 5), coupled with the expectation of reduced solubility due to the reasons above, leads to its higher selectivity over Sr^{2+}. Even so, the above solid complexes are much more "exposed" to the solvent than the earlier complexes reported for alkali metal ions (K^+, Rb^+, Cs^+), both in terms of their networked structure and also in terms of their microenvironment, which contains four coordinated water molecules.

Hydration enthalpy is another factor to consider. The hydration enthalpies of Mg^{2+}, Ca^{2+}, Sr^{2+}, and Ba^{2+} are –459.1, –376.9, –344.9, and –311.9 kcal mol^{-1}, respectively.[13] Therefore, the displacement of water from the hydrated ions is least facile for Mg^{2+} and most facile for Ba^{2+}. This would promote complex formation with DPA^- in the case of Ba^{2+}, which, in turn, would allow formation of the network structure required for precipitation. A similar trend was also observed for the alkali metal ions Na^+, K^+, Rb^+, and Cs^+. However, that the other factors alluded to above are also critically important is evident from the fact that Na^+, despite a much lower hydration enthalpy (–97 kcal mol^{-1}) than Sr^{2+} and Ba^{2+}, does not form a complex whereas the latter ions do. Moreover, the charge of the cation is also expected to play an important role in complexation. The doubly positive charge on the alkaline earth metal ions obviously attracts $O^{\delta-}$ of the ligand more strongly than monovalent cations. This stronger interaction partially compensates the opposite force due to the high hydration enthalpy of the cations in the complexation process.

Conclusion

We conclude from the present study that precipitation of alkaline earth metal ions with DPA^- requires the formation of stable assemblies. Simple salts such as $Ca(DPA)_2$, which are unable to form network structures, are highly soluble in water. Formation of such an assembly primarily depends on the ionic size, hydration enthalpy, and ionic charge. Ionic size should be such that the metal ion can fit into the cavity and provide the strong M···O interactions needed to form a stable complex. A smaller ionic size, typically ≤2.0 Å − the ionic sizes of Mg^{2+}, Ca^{2+}, and Na^+ are 1.30, 1.98, and 1.94 Å, respectively − is unfavorable for formation of this assembly. The possibility of complex formation decreases for cations having the same charge with increasing hydration enthalpy. With a mixture of cations, the selectivity depends on the ease of complex formation and the consequent structures of the assemblies: the lower the exposure of the metal ion and polar groups of the ligand to the sol-

vent (water), the higher the selectivity to precipitation. Taking both the alkali and alkaline earth metal ions jointly, the selectivity towards precipitation in the presence of DPA^- follows the overall trend: $Cs^+ > Rb^+ > K^+ > Ba^{2+} > Sr^{2+} >> Na^+, Ca^{2+}, Mg^{2+}$.

Experimental Section

Materials: Dipicrylamine was purchased from National Chemical Co., India, and was used as received. AR grade $MgCl_2$, $SrCl_2$, $BaCl_2$, and CaO were obtained from S. D. Fine Chemicals. Doubly distilled water was used for the preparation of all complexes.

Instrumentation: Elemental analyses (C, H, N) were performed on a model 2400 Perkin–Elmer elemental analyzer. Cation concentration was measured with a Dionex 500 ion chromatograph. X-ray powder diffraction data were collected with a Philips X' Pert MPD system with Cu-K_α radiation. Single-crystal structures were determined with a Bruker SMART APEX (CCD) diffractometer.

Competitive Precipitation Study with DPA^-: $Ca(DPA)_2$ was obtained by stoichiometric reaction of CaO and DPA in an aqueous medium; this compound is highly soluble in water. The Sr^{2+} complex was found to be less soluble in water and the Ba^{2+} complex is the least soluble among these salts. For the competitive precipitation study an aqueous solution of $Ca(DPA)_2$ was added to a solution containing equimolar amounts of Mg^{2+}, Sr^{2+}, and Ba^{2+}. In a typical experiment, an aqueous solution (2 mL) of $Ca(DPA)_2$ (0.25 M), obtained by the reaction of CaO (0.5 mmol) and DPA (1.0 mmol), was added to a solution (1 mL) containing a mixture of $MgCl_2$, $SrCl_2$, and $BaCl_2$ (0.5 M with respect to each metal ion). The reaction mixture was then stirred for 30 min at room temperature, and the orange precipitate thus obtained was isolated by filtration on a frit and dried in vacuo overnight to yield 488 mg (91%) of a solid with a similar powder XRD pattern to that of $[M(DPA)_2(H_2O)_4]$ (M = Ba, Sr). The precipitate was not washed with water to avoid possible dissolution of some of it. The concentrations of metal ions in the precipitate were assessed by ion chromatography. The solubility of the Sr^{2+} complex in water is significant, therefore, the amount of this complex in the precipitate obtained from the mixture of cations should decrease upon decreasing the concentration of the metal ion in the reaction mixture. Therefore, another set of experiments was conducted under similar experimental conditions, with the exception of the concentration of the metal ions – in this case 4 mL of a solution containing 0.5 mmol of each metal ion (0.125 M) was used. Yield: 485 mg (90%) with respect to DPA^-.

To estimate the relative concentrations of metal ions in the precipitate, a standard solution containing chloride salts of Mg^{2+}, Ca^{2+}, Sr^{2+}, and Ba^{2+} (20 ppm each) was analyzed by ion chromatography on an Ion Pac CS12 (2 mm) analytical column with 20 mM methylsulfonic acid as eluent (flow rate: 0.25 mL min^{-1}). Subsequently, 7.4 mg of the precipitate obtained above was dissolved in 10 mL of Milli-Q (Millipore Corporation) water and filtered through 0.2-μm filter paper. Peaks were obtained at the same retention times as above suggesting that the $[M(DPA)_2(H_2O)_4]$ complexes dissociate under dilute conditions to yield the fully hydrated ions as in the case of solutions made from the simple chloride salts. Analytical results (in mol-%) obtained for the first experiment (0.333 M of each metal ion): Ba^{2+}: 75.9; Sr^{2+}: 24.0; Mg^{2+} and Ca^{2+}: traces; for the second experiment (0.17 M of each metal ion): Ba^{2+}: 84.9; Sr^{2+}: 15.0; Mg^{2+} and Ca^{2+}: traces.

Synthesis of Metal Salts of DPA^-

$[Sr(DPA)_2(H_2O)_4]$ (1): Solid CaO (1.1 mmol, 61.7 mg) was added to DPA (2 mmol, 878 mg) suspended in water (5 mL). After 10 min of stirring at room temperature, the dark-red solution was filtered, and the filtrate containing $Ca(DPA)_2$ was added dropwise to an aqueous solution (5 mL) of $SrCl_2{\cdot}6H_2O$ (1 mmol, 266.6 mg). The reaction mixture was stirred for 1 h, during which some of the Sr^{2+} complex precipitated. The compound was separated by filtration, and the filtrate was allowed to evaporate to dryness at room temperature. After 2 d another crop of microcrystalline complex was obtained. Combined yield: 0.72 g (70%). X-ray quality crystals were obtained by slow evaporation (ca. two weeks) of an aqueous solution of the complex. $C_{24}H_{16}N_{14}O_{28}Sr$ (1036.1): calcd. C 27.82, H 1.56, N 18.93; found C 28.10, H 1.45, N 18.62.

$[Ba(DPA)_2(H_2O)_4]$ (2): This compound was synthesized following the same procedure as that described for complex **1**, except $BaCl_2{\cdot}4H_2O$ was used in place of $SrCl_2{\cdot}6H_2O$. In this case almost the entire amount of compound was precipitated during stirring, and the filtrate was not processed further to obtain another crop. Yield: 1.0 g (92%). X-ray quality crystals were obtained following the same method as that described for compound **1**. $C_{24}H_{16}BaN_{14}O_{28}$ (1085.8): calcd. C 26.54, H 1.49, N 18.06; found C 26.29, H 1.36, N 17.91.

X-ray Crystallography: Crystal data collection and refinement parameters for complexes **1** and **2** are given in Table 3. Data sets were obtained on a Bruker Smart Apex diffractometer with a CCD area detector using graphite-monochromated Mo-K_α radiation (λ = 0.71073 Å) at 100 K. Data frames were processed using the Bruker SAINT program.[14] Intensities were corrected for Lorentz, polarization, and decay effects, and an absorption correction was applied using SADABS.[15] The structure was solved by direct methods using SHELXS-97[16] and refined on F^2 using SHELXL-97.[17] The non-hydrogen atoms were located directly by successive difference Fourier calculations, and anisotropic full-matrix refinement of all atoms was carried out using SHELXL-97 until convergence was reached, which showed no significant peaks in the difference Fourier map. H-atoms attached to the phenyl rings of the DPA moiety in both the complexes were calculated on the basis of geometric criteria and were treated with a riding model in subsequent refine-

Table 3. Summary of crystallographic data for **1** and **2**.

Compound	**1**	**2**
Formula	$C_{12}H_8N_7O_{14}Sr_{0.5}$	$C_{12}H_8Ba_{0.50}N_7O_{14}$
Formula weight	518.06	542.92
a [Å]	12.1812(6)	9.1889(15)
b [Å]	12.1812(6)	9.6352(16)
c [Å]	21.8380(16)	11.697(2)
α [°]	90.00	76.106(3)
β [°]	90.00	72.734(3)
γ [°]	120.000	68.376(3)
Z	6	2
V [Å^3]	2806.2(3)	909.3(3)
Crystal system	trigonal	triclinic
Space group	$P322_1$	$P\bar{1}$
λ [Å]	0.71073	0.71073
$\rho_{calcd.}$ [g cm^{-3}]	1.839	1.983
Abs coefficient, μ [cm^{-1}]	15.68	12.23
F(000)	1560	538
Temperature [K]	100(2)	100(2)
Reflns collected/unique/R(int)	16369/4417/0.0291	5510/3990/0.0103
GOF on F^2	0.683	1.041
R_1/wR_2 [$I > 2\sigma(I)$]	0.0302/0.0762	0.0264/0.0710
R_1/wR_2 (all data)	0.0364/0.0790	0.0264/0.0710

ments using the SHELXL default parameters. Hydrogen atoms attached to the water oxygen atoms in both the complexes were located from the difference Fourier map. In the case of **1**, water hydrogen atoms were kept fixed and included only in the structure factor calculation whereas in **2** they were refined isotropically. Molecular graphics of the crystal structures were generated using ORTEP, PLATON, and Mercury.[18–20]

CCDC-610046 and -610047 (for **1** and **2**, respectively) contain the supplementary crystallographic data for this paper. These data can be obtained free of charge from The Cambridge Crystallographic Data Centre via www.ccdc.cam.ac.uk/data_request/cif.

Powder X-ray Data Collection: Powder X-ray data of the bulk precipitates of **1** and **2** were collected at room temperature in continuous scan mode in the 2θ range 5–60° with a step size of 0.02° 2θ and a count time of 4 s per step. Powder XRD patterns of **1** and **2** were also obtained by simulation from the single-crystal X-ray data using the Mercury program.[20]

Supporting Information (see footnote on the first page of this article): ORTEP views of complexes **1** (Figure S1) and **2** (Figure S2).

Acknowledgments

We are grateful to the Department of Science and Technology (DST), Government of India, for financial support. We also thank CSIR, New Delhi, for generous support towards infrastructures and core competency development. P.A. gratefully acknowledges CSIR for their award of a Senior Research Fellowship. We thank Dr. (Mrs.) P. Bhatt for the powder XRD measurements.

[1] K. Wozniak, P. R. Mallinson, C. C. Wilson, E. Hovestreydt, E. Grech, *J. Phys. Chem. A* **2002**, *106*, 6897.
[2] a) K. Wozniak, H. He, J. Klinowski, W. Jones, E. Grech, *J. Phys. Chem.* **1994**, *98*, 13755; b) M. L. Kundu, J. N. Kapoor, S. K. Ghosh, *Proc. Indian Acad. Sci. (Chem. Sci.)* **1982**, *91*, 65.
[3] A. Winkel, D. I. H. Maas, *Angew. Chem.* **1936**, *49*, 827.
[4] a) J. Kielland, *Patent*, **1940**, No. Au 109552 19400110; **1941**, No. DE 715199 19411120; b) J. Kielland, W. Fleischer, *Patent*, **1940**, No. AU 112196 19401219; c) E. Berner, J. Kielland, *Patent*, **1942**, No. DE 726545 19420903; d) F. Massazza, B. Riva, *Ann. Chim. (Rome)* **1958**, *48*, 664; e) F. Massazza, B. Riva, *Ann. Chim. (Rome)* **1961**, *51*, 645; f) J. N. Kapoor, J. M. Sarkar, *Technology (Sindri, India)* **1966**, *3*, 177; g) S.-K. Chu, C.-T. Liaw, *Huaxue* **1969**, *4*, 106; h) J. Kielland, *Chem. Ind. (London)* **1971**, 1309; i) M. Y. Bakr, A. A. Zatout, *Chem. Econ. Eng. Rev.* **1979**, *11*, 31.
[5] V. Kourim, J. Krtil, *Proceedings of the UN International Conference on the Peaceful Uses of Atomic Energy*, 2nd meeting, Geneva, **1958**, *28*, 139.
[6] J. Rais, P. Selucky, *Patent*, **1973**, No. CZXXA9 CS 149403 19730715.
[7] L. A. Bray, E. C. Martin, R. L. Moore, W. A. Richland, *U.S. At. Energy Commun.* **1962**, *##HW-SA-2620*, 8.
[8] E. Suresh, P. Agnihotri, B. Ganguly, P. Bhatt, P. S. Subramanian, P. Paul, P. K. Ghosh, *Eur. J. Inorg. Chem.* **2005**, 2198.
[9] P. Paul, P. K. Ghosh, K. J. Langalia, P. S. Subramanian, E. Suresh, S. Patra, P. Agnihotri, *Patent (applied, PCT and USA)*, **2005**, Application No. 0312NF2005.
[10] P. D. Beer, P. A. Gale, Z. Chen, M. G. B. Drew, J. A. Heath, M. I. Ogden, H. R. Powell, *Inorg. Chem.* **1997**, *36*, 5880.
[11] G. Mezei, R. G. Raptis, *New J. Chem.* **2003**, *27*, 1399.
[12] C. J. Pedersen, *J. Am. Chem. Soc.* **1967**, *89*, 7017.
[13] F. A. Cotton, W. Wilkinson, *Advanced Inorganic Chemistry, A comprehensive Text*, 3rd Ed., **1979**, pp. 198 and 645.
[14] Bruker Analytical X-ray Instruments, Inc., Madison, WI.
[15] G. M. Sheldrick, University of Göttingen, Göttingen, Germany, **1996**.
[16] G. M. Sheldrick, *SHELXS97, a program for crystal structure solution*, University of Göttingen, Germany, **1997**.
[17] G. M. Sheldrick, *SHELXL97, a program for crystal structure refinement*, University of Göttingen, Germany, **1997**.
[18] C. K. Johnson, *ORTEP II, Report ORNL-5138*, Oak Ridge National Laboratory, Oak Ridge, TN, **1976**.
[19] A. L. Spek, *PLATON-97*, University of Utrecht, Utrecht, The Netherlands, **1997**.
[20] *Mercury 1.3*, Supplied with Cambridge Structural Database CCDC, Cambridge, U. K., **2003–2004**.

Received: July 14, 2006
Published Online: October 12, 2006

